

Static and Dynamic Mechanical Properties of Flame-Retardant Copolyester/Nano-ZnCO₃ Composites

Haiming Liu,¹ Rui Wang,² Xi Xu¹

¹State Key Laboratory of Polymer Materials Engineering, Department of Polymer Science and Materials, Sichuan University, Chengdu 610065, China

²Department of Materials Science and Engineering, Beijing Institute of Fashion Technology, Beijing 100029, China

Received 8 April 2010; accepted 28 October 2010

DOI 10.1002/app.33632

Published online 6 April 2011 in Wiley Online Library (wileyonlinelibrary.com).

ABSTRACT: Novel phosphorus-containing copolyester nanocomposites were synthesized by *in situ* polymerization with 2-carboxyethyl(phenylphosphinic) acid (CEPPA) and nano-ZnCO₃. The flame retardancy and static and dynamic mechanical properties of poly(ethylene terephthalate) (PET)/nano-ZnCO₃ composites and phosphorus-containing copolyester/nano-ZnCO₃ composites were evaluated with limiting oxygen index measurements, vertical burning testing (UL-94), a universal tensile machine, and a dynamic mechanical analysis thermal analyzer. The phosphorus-containing copolyester nanocomposites had higher limiting oxygen indices (ca. 32%) and a V0 rating according to the UL-94 test; this indicated that nano-ZnCO₃ and CEPPA greatly improved the flame retardancy of PET. The static mechanical test results showed that the breaking strength, modulus, and yield stress of the composites tended to increase with increasing nano-ZnCO₃ content; when 3 wt % nano-ZnCO₃ was added to PET and the phosphorus-containing copolyester, the breaking

strength of the composites was higher than that of pure PET. Dynamic mechanical analysis indicated that the dynamic storage modulus and loss modulus of the PET composites increased markedly in comparison with those of pure PET. However, the glass-transition temperatures associated with the peaks of the storage modulus, mechanical loss factor, and loss modulus significantly decreased with the addition of ZnCO₃ and CEPPA. The morphologies of the composites were also investigated with scanning electron microscopy, which revealed that nano-ZnCO₃ was dispersed homogeneously in the PET and copolyester matrix without the formation of large aggregates. In addition, the interfacial adhesion of nano-ZnCO₃ and the matrix was perfect, and this might have significantly affected the mechanical properties of the composites. © 2011 Wiley Periodicals, Inc. *J Appl Polym Sci* 121: 3131–3136, 2011

Key words: blends; mechanical properties; nanocomposites; polyesters

INTRODUCTION

Poly(ethylene terephthalate) (PET) is a semicrystalline, thermoplastic resin used in a wide range of applications, such as flooring, surface coatings, electrical equipment, automobiles, and textiles, because of its good mechanical and optical properties, excellent flow characteristics, and low cost.^{1–3} However, high-performance applications in some special fields such as transportation, rubber tire manufacturing, and building require PET to have good flame retardancy, high thermal stability, high modulus, and other high mechanical properties. With respect to the nanosize effect of nanoparticles, many researchers have been trying to improve the flame retardancy and mechanical properties of polymers through the combination of phosphorus-containing flame retardants and nanoparticles. Many studies have

shown that adding phosphorus-containing flame retardants and nanoparticles to polyesters is one of the most efficient methods; it imparts good flame retardancy and high mechanical properties to polyesters and can simultaneously minimize the negative impact on the physical and chemical properties of polymers.^{4–8} Therefore, flame-retardant polymer nanocomposites (especially reinforced ones) have been attracting more and more attention because nanoparticles have special surface effects, small size effects, and quantum effects. Conventional nanofillers, which are extensively used in the polymer industry, include montmorillonite clay,⁷ silica,⁴ nano-SiO₂,^{9,10} and nano-TiO₂,¹¹ among others. Many studies have shown that polymer properties are considerably enhanced by the incorporation of nanofillers. Their composites exhibit excellent thermal, mechanical, barrier, and other properties because of uniform filler dispersion, strong interfacial forces between a nanometer-sized filler and a polymer, slipping effects, and nanoparticle lubrication.^{6,7,12,13}

Dynamic mechanical test methods have been widely employed for investigating the structures and viscoelastic behavior of polymeric materials to

Correspondence to: R. Wang (wangrui166@sohu.com).

Contract grant sponsor: China Petroleum and Chemical Corp.; contract grant number: 206031.

determine their relevant stiffness and damping characteristics for some kinds of applications.^{14–19} The introduction of phosphorus-containing flame retardants and reinforcing fillers into polymers probably affects the storage modulus (E'), loss modulus (E''), and glass-transition temperature (T_g). Therefore, it is necessary to evaluate the effects of nanofillers on the dynamic mechanical properties of polymer composites. To the best of our knowledge, there are few reports about the introduction of 2-carboxyethyl(phenylphosphinic) acid (CEPPA) and nano-ZnCO₃ into polyesters and the dynamic mechanical properties of phosphorus-containing copolyester/nano-ZnCO₃ composites. Thus, in this study, a series of PET/nano-ZnCO₃ composites and phosphorus-containing copolyester/nano-ZnCO₃ composites were synthesized by *in situ* polymerization with CEPPA and nano-ZnCO₃. The flame retardancy and static and dynamic mechanical properties of the resulting composites were investigated. The morphologies of the composites were also characterized with scanning electron microscopy (SEM) so that we could further understand the effects of nano-ZnCO₃ and CEPPA on the mechanical properties of the composites.

EXPERIMENTAL

Materials

Nano-ZnCO₃ was purchased from Nanjing Haitai Nano Co., Ltd. (Nanjing, China), and its mean particle size was 50 nm. Terephthalic acid, ethylene glycol (EG), and Sb₂O₃ were donated by Sinopec Tianjin Petrochemical Co., Ltd. (Tianjin, China). CEPPA was supplied by Sinopharm Chemical Reagent Beijing Co., Ltd. (Beijing, China). All other materials were commercially available.

Synthesis of the phosphorus-containing copolyester/nano-ZnCO₃ composites

CEPPA was first reacted with EG (1:2 molar ratio) at 100°C for 3 h to produce CEPPA–EG with higher thermal performance and reactivity. Then, terephthalic acid, EG, CEPPA–EG, Sb₂O₃, and mechanically ball-milled nano-ZnCO₃ were added to a 1500-mL, four-necked, round-bottom flask equipped with a thermometer and a mechanical stirrer. The mixture was heated to 250°C and was maintained between 250 and 260°C until the conversion of this esterification reached 96%. Then, the esterification products were transferred to a 1.0-L reactor equipped with a nitrogen inlet, a condenser, and a mechanical stirrer. The reactor was fitted to a vacuum system and evacuated for the removal of all oxygen. The reactor was then heated to 280–285°C under a pressure of less than 50 Pa, and this was maintained for 2 to 3 h to produce phosphorus-containing copolyester nanocomposites. Finally,

the resulting polymer melts were extruded at the pressure of N₂ and cooled with water after the heat and vacuum were removed. Thus, PET nanocomposites containing different amounts of nano-ZnCO₃ were synthesized. Subsequently, all extruded, strip-shaped materials were pelletized for further characterization.

Characterization

The flame retardancy of PET and PET composites was characterized with the limiting oxygen index (LOI) and vertical burning tests (UL-94). The LOI values were measured on a JF-3 oxygen index meter (Jiangning Nanjing Analytical Instrument Factory, Jiangning, China) according to ASTM D 2863 with sheet dimensions of 100 × 6.5 × 3.0 mm³. The vertical burning tests were conducted on a CZF-3 instrument (Jiangning Nanjing Analytical Instrument Factory, Jiangning, China) according to the ASTM D 3801 testing procedure with sheet dimensions of 130 × 12.5 × 3.0 mm³.

PET composites were dried in a vacuum oven at 150°C for over 10 h for the removal of excess moisture. The dried composites were subsequently compression-molded into tensile dumbbell specimens with sheet dimensions of 28 × 3.2 × 2.8 mm³ before tensile testing was performed. The tensile tests were carried out with a universal testing machine (Instron, Norwood, Massachusetts, United States) at a head speed of 100 mm/min. All measurements were repeated five times, and the values were averaged. All mechanical properties were performed at room temperature.

A Q800 dynamic mechanical analysis thermal analyzer (TA Instruments, New Castle, Delaware, United States) was used to measure the dynamic mechanical properties of the specimens. A dual-cantilever clamp and a dynamic mechanical analysis multifrequency strain module were used. The measurements were performed from 25 to 200°C at a heating rate of 3°C/min and at a fixed frequency of 1.0 Hz with sheet dimensions of 65.0 × 6.5 × 2.4 mm³.

SEM was performed on a JSM-6360 scanning electron microscope (JEOL, Tokyo, Japan) at the operating voltage of 10 kV. Nano-ZnCO₃ was treated in EG, and then the dispersed solution was dried and coated with a thin layer of gold before it was placed in the scanning electron microscope. PET/nano-ZnCO₃ composites were snapped in two in liquid nitrogen, and then the fractures of the specimens were coated with a thin layer of gold before they were placed in the scanning electron microscope.

RESULTS AND DISCUSSION

Flame retardancy of the PET composites

LOI measurements and UL-94 testing are widely used to evaluate the flame-retardant properties of

TABLE I
LOI and UL-94 Test Results

Sample	Phosphorus (wt %)	ZnCO ₃ (wt %)	LOI (vol %)	Dripping	UL-94 rating
PET	0	0	23	Yes	V2
PET01	0	0	22	Yes	V2
PET02	0	0	24	Yes	V2
PET03	0	0	25	Yes	V2
PET60	0.6	0	29	Yes	V0
PET61	0.6	1.0	32	Yes	V0
PET62	0.6	2.0	31	Yes	V0
PET63	0.6	3.0	32	Yes	V0

materials. The corresponding LOI values and UL-94 ratings are listed in Table I. Pure PET had an LOI value of only 23% and a V2 rating according to the UL-94 test, whereas PET60, which contained 0.6 wt % phosphorus, had a much higher LOI value (29%) and reached a V0 rating; this indicated that phosphorus had a significant effect on the improvement of the flame retardancy of PET. This phenomenon might be attributed to the introduction of CEPPA, which catalyzed char formation; the char in turn inhibited the combustion and decomposition of PET, and this enhanced the LOI value and UL-94 rating.¹⁷ The LOI values of the PET/nano-ZnCO₃ composites slightly increased with the nano-ZnCO₃ content increasing up to 3 wt %; when 3 wt % nano-ZnCO₃ was added to the PET matrix, the LOI value increased from 23 to 25%. The LOI values of the PET/nano-ZnCO₃ composites were nearly the same as the value of pure PET. Moreover, the PET/nano-ZnCO₃ composites achieved only a V2 rating according to the UL-94 test, and this revealed that nano-ZnCO₃ had little effect on the flame retardancy and antidripping properties of the composites. However, the LOI values of the phosphorus-containing copolyester/nano-ZnCO₃ composites increased to approximately 32% and were considerably higher than those of PET and the PET/nano-ZnCO₃ composites. Obviously, the combination of nano-ZnCO₃ and phosphorus effectively improved the flame retardancy of PET in comparison with pure PET and the PET/nano-ZnCO₃ composites. The results also show that phosphorus and nano-ZnCO₃ had some synergistic flame-retardant effects on PET, which might have been due to the char-forming mechanism of CEPPA^{20–22} and the good dispersion and small size of the nano-ZnCO₃ particles.^{22–24}

Static mechanical properties

The mechanical properties of PET were affected by the incorporation of CEPPA and nano-ZnCO₃. The results for the static mechanical properties of the PET/nano-ZnCO₃ composites and the phosphorus-containing copolyester nanocomposites are listed in

TABLE II
Static Mechanical Properties of the PET Composites

Sample	Yield stress (MPa)	Breaking strength (MPa)	Modulus (MPa)	Breaking elongation (%)
PET	48.6	24.0	1760	205
PET01	48.2	19.7	1850	174
PET02	49.2	22.8	1886	210
PET03	47.9	24.4	1843	209
PET60	48.0	26.7	1900	170
PET61	53.9	21.6	1960	171
PET62	54.1	23.1	1920	160
PET63	52.3	24.7	1883	162

Table II. Figure 1 shows the behavior of the PET composites during stretching, and it was similar to the behavior of pure PET. Typical tensile stress-strain curves for all the samples were obtained. They revealed that the mechanical behavior was typical for pure PET: stress whitening followed by necking and stretching. The tensile strength at break of the PET/nano-ZnCO₃ composites and phosphorus-containing copolyester/nano-ZnCO₃ composites increased with increasing nano-ZnCO₃ content. When less than 2 wt % nano-ZnCO₃ was added, the tensile strength at break of the PET/nano-ZnCO₃ composites and phosphorus-containing copolyester/nano-ZnCO₃ composites was lower than that of neat PET. However, when 3 wt % nano-ZnCO₃ was added to the PET and phosphorus-containing copolyester matrix, the breaking strength of the composites (PET03 and PET63) was higher than that of pure PET. This probably occurred because the slipping effect of the nanoparticles played a dominant role and the adhesion of nano-ZnCO₃ to the matrix had little effect on the breaking strength when less than 3 wt % nano-ZnCO₃ was added.^{13,19} In comparison with pure PET, the breaking strength of PET60 increased from 24.0 to 26.7 MPa, and the modulus of PET60 increased from 1760 to 1900 MPa. Phosphorus

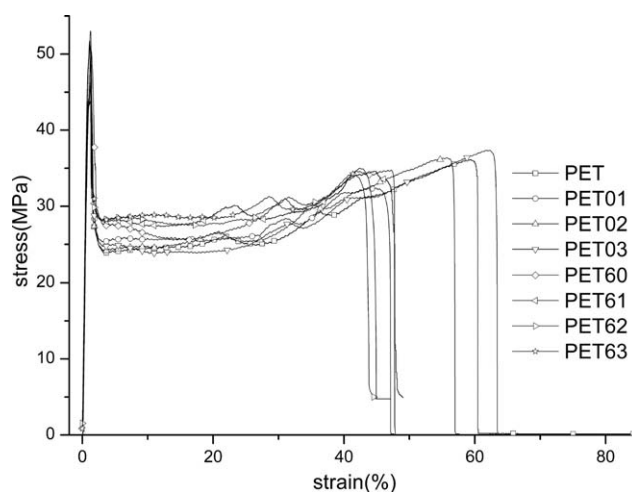


Figure 1 Tensile stress-strain curves for the PET composites.

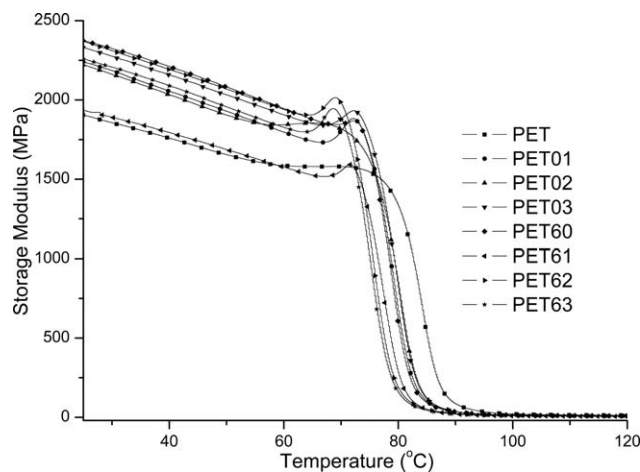


Figure 2 E' as a function of temperature for the PET composites.

increased the breaking strength and modulus of PET, and this possibly occurred because the flexible chain segments formed by the CEPPA block absorbed energy during the stretching process. In addition, the addition of nano-ZnCO₃ significantly improved the initial modulus and yield stress of the composites because of the stiffness of nano-ZnCO₃ and the good interfacial adhesion between nano-ZnCO₃ and PET. This phenomenon can be explained by the strengthening and toughening mechanism of inorganic fillers.²⁵ Moreover, the uniform dispersion of nano-ZnCO₃ in the PET nanocomposites and the good interfacial adhesion between nano-ZnCO₃ and the PET matrix could produce notable improvements in the modulus and yield stress. The static mechanical properties suggest that the combination of CEPPA and nano-ZnCO₃ could be used to impart good flame retardancy to PET with high mechanical properties.^{26,27}

Dynamic mechanical properties

The dynamic mechanical properties of the phosphorus-containing copolyester and its composites, such as E' , E'' , and the mechanical loss factor ($\tan \delta$), were studied as a function of temperature and are shown in Figures 2–4; the corresponding test results are summarized in Table III. Figure 2 compares the trend of E' versus the temperature between 25 and 140°C. The E' curves go through a maximum in the glass-transition region, in which the free volume reached a critical level.¹⁹ This happened because nanoparticles, dispersed uniformly in the polyester matrix, acted as physical entanglement points of the molecular chain, and this limited chain flexibility and mobility. In addition, the physical entanglement points formed by the CEPPA block also restrained the free movement of chain segments. When the temperature increased, the number of entanglement

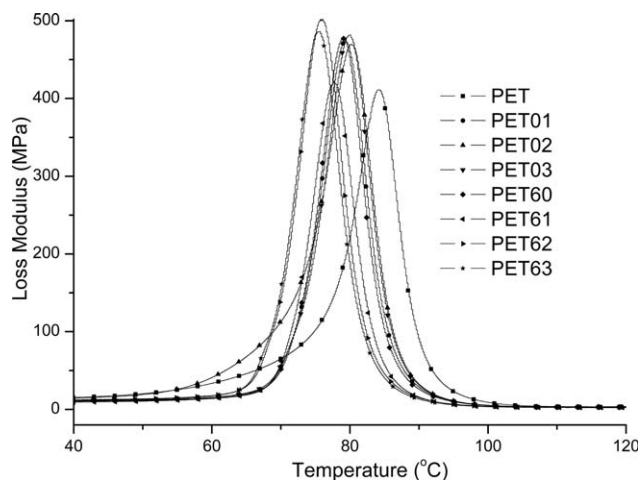


Figure 3 E'' as a function of temperature for the PET composites.

points and their entanglement role were enhanced, and the internal friction of the polymer also increased. Therefore, the chain flexibility and chain mobility gradually decreased, and this caused E' of the polymers to increase. When the temperature increased to a certain degree, the chain flexibility and mobility approached a minimum value; meanwhile, E' of the polymers achieved a relative maximum value. As the temperature continued to increase, the molecular chains obtained enough energy to overcome the friction resistance, and the entire chain segments could move freely; this caused a rapid decline in E' .²⁶

Table III also shows that E' of PET60 increased to 1858 MPa, and this can be attributed to the entanglement points formed by the flexible chain segments of the CEPPA block. E' of PET61 was nearly the same as that of pure PET. This can be explained as follows. First, the slipping effect of the nanoparticles

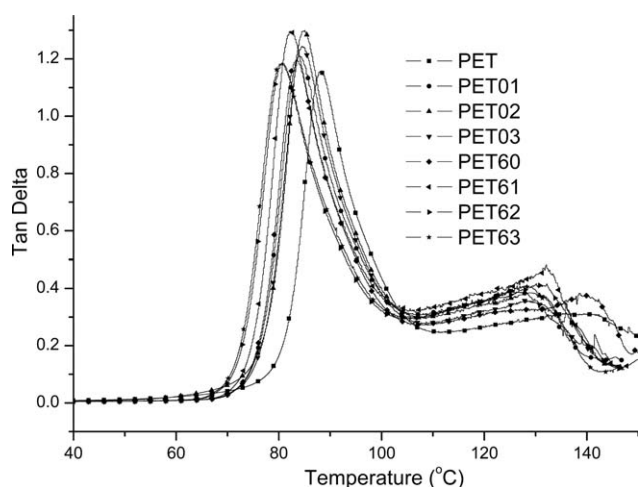


Figure 4 $\tan \delta$ as a function of temperature for the PET composites.

TABLE III
Dynamic Mechanical Properties of the PET Composites

Sample	$T_{g,E'}$ (°C)	E' (MPa)	$T_{g,E''}$ (°C)	E'' (MPa)	T_{g,δ_1} (°C)	Tan δ_1	T_{g,δ_2} (°C)	Tan δ_2
PET	80	1580	84	411	88	1.16	137	0.31
PET01	72	1884	79	472	84	1.21	125	0.38
PET02	65	1855	80	470	85	1.30	129	0.38
PET03	72	1934	80	482	84	1.24	128	0.35
PET60	72	1858	79	479	83	1.20	139	0.38
PET61	71	1583	78	416	82	1.30	132	0.48
PET62	69	2016	76	501	81	1.18	131	0.42
PET63	69	1945	75	486	81	1.19	128	0.41

played a dominant role. Second, the adhesion of nano-ZnCO₃ to the matrix had little effect on E' when less than 2 wt % nano-ZnCO₃ was added. Finally, the phosphorus-containing chain segment was of little value to the improvement of the modulus. When more than 2 wt % nano-ZnCO₃ was added, the modulus of the phosphorus-containing copolyester nanocomposites was higher than the modulus of pure PET because of the high modulus of nano-ZnCO₃, the good interfacial adhesion due to the interaction between ZnCO₃ and the matrix, and the contribution of the phosphorus-containing chain segment to the improvement of the modulus. Furthermore, the introduction of nano-ZnCO₃ and CEPPA into the polyester improved the flexibility of the molecular chains, and this caused $T_{g,E'}$, $T_{g,E''}$, and T_{g,δ_1} of the composites to decrease; they were lower than those of pure PET. T_g of the nano-ZnCO₃ composites decreased with the content of ZnCO₃ increasing, and this was related to slipping effects and lubrication of the nanoparticles.²⁷

The trends of the dissipative component of the dynamic modulus (E'') as a function of the temperature are reported in Figure 3. In the glass-transition region, the E'' and tan δ curves go through a maximum. This behavior can be attributed to internal friction and disentanglement effects of the nanoparticles. The temperature dependence of tan δ of the copolyester nanocomposites is shown in Figure 4. Tan δ reached a maximum value in the glass-transition region. Furthermore, tan δ of the composites shifted slightly and was higher than that of pure PET; this indicated that the internal friction resistance of the composites was higher than that of pure PET. The tan δ values of all samples were greater than 1.0, and this indicated that E'' was higher than E' in the glass-transition region. The values of tan δ decreased with the content of ZnCO₃ because of the slipping effect of the nanoparticles and reduced friction of the PET composites.²⁴ After the glass transition, a considerable increase in tan δ was observed between 130 and 180°C and could be attributed to partial crystallization caused by the increase in the mobility of the polymer chains after T_g . Meanwhile, the T_{g,δ_2} values of the PET/nano-ZnCO₃ composites and phosphorus-

containing copolyester composites were lower than the value of pure PET because nano-ZnCO₃, acting as a nucleating agent, accelerated the crystallization.¹⁰

Morphology of the composites

Many studies of thermoplastic nanocomposites have revealed that the interfacial adhesion and dispersion characteristics of nanoparticles in composites are greatly responsible for the reinforcement effect of polymer nanocomposites, and they also significantly affect the final mechanical properties (e.g., the modulus and strength).^{13,17,19} To determine the relationship between the morphology of PET/nano-ZnCO₃ composites and their mechanical properties, we studied the morphology and nano-ZnCO₃ distribution in the PET and phosphorus-containing copolyester matrix with SEM. Figure 5(a) shows the morphology of nano-ZnCO₃, and Figure 5(b–f) shows the morphology of pure PET and PET/nano-ZnCO₃ composites. As shown in Figure 5(a), nano-ZnCO₃ was dispersed uniformly in EG, its size ranging from 50 to 500 nm. Figure 5(c,d) shows that the size of the nano-ZnCO₃ particles in the PET matrix ranged from 50 to 500 nm. Moreover, all these samples showed a uniform distribution of nano-ZnCO₃ particles in the PET and PET composite matrix. There were no large aggregates of nano-ZnCO₃ in the PET and PET composite matrix. As shown in Figure 5(d), PET63 had good interfacial adhesion between nano-ZnCO₃ and the PET matrix, and this contributed to the increase in the modulus and breaking strength.¹⁹

CONCLUSIONS

In this work, phosphorus-containing copolyester nanocomposites were synthesized by *in situ* polymerization with CEPPA and nano-ZnCO₃. The combination of CEPPA and nano-ZnCO₃ could be used to impart good flame retardancy to PET with high mechanical properties. The phosphorus-containing copolyester nanocomposites had a higher LOI value (ca. 32%) and a V0 rating according to the UL-94 test. The static mechanical test results showed that

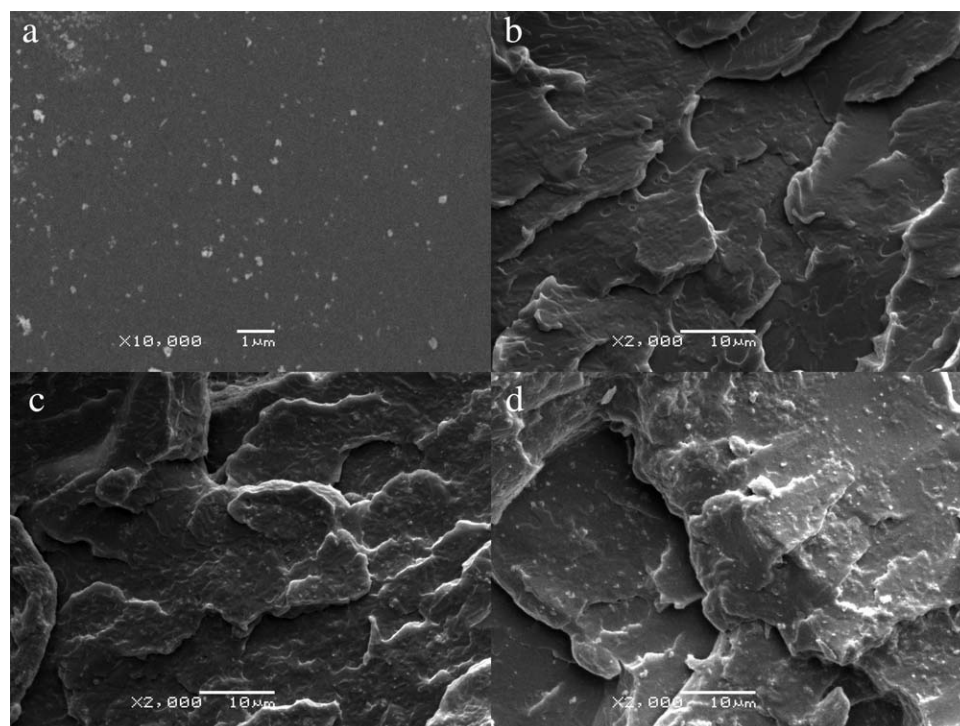


Figure 5 SEM images of (a) nano-ZnCO₃ dispersed in EG and (b–d) fracture surfaces of PET, PET03, and PET63, respectively.

the breaking strength, modulus, and yield stress of the composites tended to increase with increasing nano-ZnCO₃ content; when 3 wt % nano-ZnCO₃ was added to PET and the phosphorus-containing copolyester, the breaking strength of the composites was higher than that of pure PET. Dynamic mechanical analysis results indicated that E' and E'' of the PET composites increased markedly in comparison with those of pure PET. However, the T_g values associated with the peaks of E' , $\tan \delta$, and E'' significantly decreased with the addition of ZnCO₃ and CEPPA. SEM observations revealed that nano-ZnCO₃ was dispersed homogeneously in the PET and copolyester matrix without the formation of big aggregates. In addition, the interfacial adhesion between nano-ZnCO₃ and the matrix was perfect, and this might have significantly affected the mechanical properties of the composites.

References

- Vlad-Bubulac, T.; Hamciuc, C.; Petreus, O. *High Perform Polym* 2006, 18, 255.
- Skinner, G. J. *Therm Anal Calorim* 2000, 59, 395.
- Asrar, J.; Berger, P.; Hurlbut, J. *J Polym Sci Part A: Polym Chem* 1999, 37, 3119.
- Fu, M.; Qu, B. *Polym Degrad Stab* 2004, 85, 633.
- Chiu, Y.; Liu, F.; Ma, C.; Chou, I.; Riang, L.; Chiang, C.; Yang, J. *Thermochim Acta* 2008, 473, 7.
- Leu, T.; Wang, C. *J Appl Polym Sci* 2004, 92, 410.
- Wang, D.-Y.; Wang, Y.-Z.; Wang, J.-S.; Chen, D.-Q.; Zhou, Q.; Yang, B.; Li, W.-Y. *Polym Degrad Stab* 2005, 87, 171.
- Katsikis, N.; Zahradnik, F.; Helmschrott, A.; Münstedt, H.; Vital, A. *Polym Degrad Stab* 2007, 92, 1966.
- Wu, T.; Ke, Y. *Polym Degrad Stab* 2006, 91, 2205.
- Ke, Y.; Wu, T.; Xia, Y. *Polymer* 2007, 48, 3324.
- Chen, J.; Dai, C.; Chen, H.; Chien, P.; Chiu, W. *J Colloid Interface Sci* 2007, 308, 81.
- Calcagno, C. I. W.; Mariani, C. M.; Teixeira, S. R.; Mauler, R. S. *Compos Sci Technol* 2008, 68, 2193.
- Wang, L.; Chen, G. *J Appl Polym Sci* 2010, 116, 2029.
- Sreekumar, P. A.; Saiah, R.; Saiter, J. M.; Leblanc, N.; Joseph, K.; Unnikrishnan, G.; Thomas, S. *Polym Compos* 2009, 30, 768.
- Mohanty, S.; Nayak, S. K. *Polym Compos* 2007, 28, 153.
- Kim, I.-H.; Jeong, Y. G. *J Polym Sci Part B: Polym Phys* 2010, 48, 850.
- Yu, X.-B.; Wei, C.; Zhang, F.-A. *Polym Adv Technol* 2006, 17, 534.
- Sakuma, T.; Kumagai, A.; Teramoto, N.; Shibata, M. *J Appl Polym Sci* 2008, 107, 2159.
- Goyal, R. K.; Tiwari, A. N.; Mulik, U. P.; Negi, Y. S. *J Appl Polym Sci* 2007, 104, 568.
- Liu, W.; Chen, D.; Wang, Y.; Wang, D.; Qu, M. *Polym Degrad Stab* 2007, 92, 1046.
- Green, J. *J Fire Sci* 1992, 10, 470.
- Hippi, U.; Mattila, J.; Korhonen, M.; Seppälä, J. *Polymer* 2003, 44, 1193.
- Gui, H.; Zhang, X.; Liu, Y.; Dong, W.; Wang, Q.; Gao, J.; Song, Z.; Lai, J.; Qiao, J. *Compos Sci Technol* 2007, 67, 974.
- Kashiwagi, T.; Morgan, A.; Antonucci, J.; VanLandingham, M.; Harris, R., Jr.; Awad, W.; Shields, J. *J Appl Polym Sci* 2003, 89, 2072.
- Ou, Y. C. *Polym Mater Sci Eng* 1998, 12, 12.
- Li, Q.; Jiang, P.; Wei, P. *J Polym Sci Part B: Polym Phys* 2005, 43, 2548.
- Russo, P.; Acierio, D.; Gallo, E. *Macromol Symp* 2009, 286, 172.